GA–A25748

LITHIUM POLARIZATION SPECTROSCOPY: MAKING PRECISION PLASMA CURRENT MEASUREMENTS IN THE DIII-D NATIONAL FUSION FACILITY

by
D.M. THOMAS

APRIL 2007

GENERAL ATOMICS

DISCLAIMER

GA–A25748

LITHIUM POLARIZATION SPECTROSCOPY: MAKING PRECISION PLASMA CURRENT MEASUREMENTS IN THE DIII-D NATIONAL FUSION FACILITY

by
D.M. THOMAS

This is a preprint of a paper to be presented at the 15th Int. Conf. on Atomic Processes in Plasma, March 19-22, 2007, in Gaithersburg, Maryland, and to be published in the *Proceedings.*

Work supported by
the U.S. Department of Energy
under DE-AC03-89ER51114 and DE-FC02-04ER54698

GENERAL ATOMICS PROJECT 30200
APRIL 2007

Lithium Polarization Spectroscopy: Making Precision Plasma Current Measurements in the DIII-D National Fusion Facility

D.M. Thomas

General Atomics, P.O. Box 85608, San Diego, California 92186-5608, USA

Abstract. Due to several favorable atomic properties (including a simple spectral structure, the existence of a visible resonance line, large excitation cross section, and ease of beam formation), beams of atomic lithium have been used for many years to diagnose various plasma parameters. Using techniques of active (beam-based) spectroscopy, lithium beams can provide localized measurements of plasma density, ion temperature and impurity concentration, plasma fluctuations, and intrinsic magnetic fields. In this paper we present recent results on polarization spectroscopy from the LIBEAM diagnostic, a 30 keV, multi-mA lithium beam system deployed on the DIII-D National Fusion Facility tokamak. In particular, by utilizing the Zeeman splitting and known polarization characteristics of the collisionally excited 670.8 nm Li resonance line we are able to measure accurately the spatio-temporal dependence of the edge current density, a parameter of basic importance to the stability of high performance tokamaks. We discuss the basic atomic beam performance, spectral line-shape filtering, and polarization analysis requirements that were necessary to attain such measurements. Observations made under a variety of plasma conditions have demonstrated the close relationship between the edge current and plasma pressure, as expected from neoclassical theory.

Keywords: plasma diagnostics, lithium beam, polarization spectroscopy, Zeeman effect, current density, tokamak edge confinement
PACS: 52.70.-m, 52.70.Kz, 52.59.Sa, 52.59.Bi, 52.40.Mj,52.20.Hv, 32.60.+I,32.70.Jz, 39.10.+j

1. INTRODUCTION

The edge current density j is an important parameter in toroidal magnetic plasma confinement experiments because it seems to be a key player in the formation and stability of the plasma pedestal. This is a region of enhanced confinement that can be established at the outer edge of the plasma, just inside the transition between open and closed magnetic field lines (Fig. 1). The height of the pedestal pressure appears to be closely related to the performance of the plasma as a whole in terms of overall (core) plasma pressure or effective fusion power. However, the pedestal pressure is limited by various magnetohydrodynamic (MHD) instabilities that can cause the collapse of the good confinement. These MHD modes may be stabilized or destabilized by the existence of neoclassical currents that are self-consistently generated by the pressure gradient in a toroidal geometry. The current and pressure are interrelated in a very complex fashion on very small spatial (10^{-3}–10^{-2} m) and (10^{-3}-10^{-1} s) temporal scales.

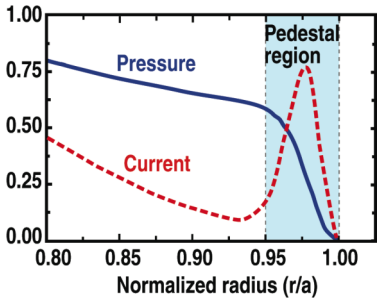

Figure 1. Edge region of a plasma with improved confinement, showing large pressure gradient and associated current peak.

While we can measure the ion and electron components of the plasma pressure with good accuracy using such techniques as Thomson scattering and charge exchange recombination spectroscopy, measurements of *j* are more difficult. One way to do this is to provide a fine scale profile of the poloidal magnetic field B_{POL} generated by the current. This must be done in the presence of the much larger toroidal magnetic field B_{TOR}. The spatial derivative of B_{POL} can then be used to infer *j* via Ampere's law. Due to the high power densities in the edges of present-day experiments, measurements using physical magnetic probes are only possible outside of the last closed flux surface and can only yield limited information on the interior structure of the underlying current distribution. More recently, measurements of the plasma internal magnetic fields have been made successfully using the motional Stark effect (MSE) [1] on fast beams of atomic hydrogen injected into the plasma. In the frame of the hydrogen atoms, the equivalent radial electric field due to the beam velocity crossed into the local B field is sufficient to split and polarize the Balmer alpha beam emission, which can then be used to determine the magnetic field components. Unfortunately, this technique is hampered by the existence of large intrinsic radial electric fields, which can result in degenerate or incorrect solutions for the true poloidal magnetic field [2]. In addition, the experiments to date have not had sufficiently fine spatial resolution to accurately analyze the local structure of the current density in the pedestal.

We have overcome these difficulties by using combined polarization and spectroscopic analysis of the resonance emission of an injected beam of lithium atoms. Because of the intrinsic (Tesla-scale) magnetic fields, the Zeeman effect splits and polarizes this resonance radiation in a known fashion. Measurements of the local magnetic field structure can be extracted in various ways from the proper analysis of this radiation. Using this technique we have been successful in making precision measurements of the current density profile in the pedestal region on the DIII-D tokamak. In this paper we will examine the various atomic physics aspects that make lithium such an attractive candidate for these measurements as well as showing some recent results of our investigations on DIII-D.

2. ADVANTAGES OF LITHIUM ATOMIC SYSTEM FOR EDGE PLASMA MEASUREMENTS

In this section we review several specific features of lithium that make it uniquely suited for measurements on modern tokamak edge plasmas.

2.1. Large Excitation Rate

Figure 2 shows a simplified level diagram for the neutral lithium system. For beam energies of a few tens of keV, the resonant 2^2S-2^2P transition is very efficiently pumped by plasma electron and ion collisions [3] (Fig. 3). Since the excitation rate for the lithium resonance line is much higher than for the hydrogen lines (500x in the case of H_α) for electron temperatures typical of the plasma edge (T_e > ~20 eV), a very small (1 cm-scale) beam can be used for probing the plasma while still providing a reasonable signal level. This can significantly improve the spatial resolution of the measurement. Although the electron loss (ionization and charge exchange) cross sections for lithium are also correspondingly large, the attenuation target thicknesses $\pi = \int ndl$ are on the order of 10^{17}-10^{18} m^{-2}. For typical edge plasma densities of a few 10^{19} m^{-3}, this is more than enough to probe the plasma pedestal region.

2.2. Transition Wavelength

The 670 nm resonance wavelength is in the visible region of the spectrum, simplifying the optical requirements for observing the fluorescence. It is also near the peak of the quantum efficiency curve for common optical detectors. Fortuitously it also resides in a region of the plasma emission spectrum having few competing lines. In addition, the relatively long wavelength results in a correspondingly large Zeeman splitting (below). Finally, because of the exceedingly short time (~10^{-15} s) associated with electron dipole emission for a single atom, for reasonable beam energies the polarization and spectral characteristics are determined by the local plasma conditions at the emission location, with no time-of-flight broadening or averaging.

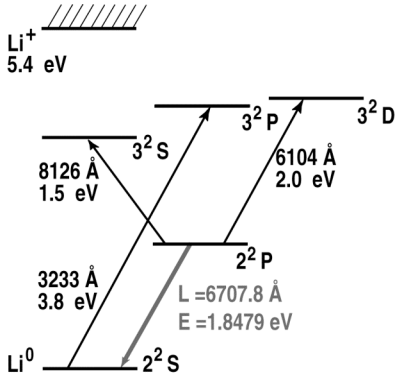

FIGURE 2. Simplified Grotrian diagram for neutral lithium system, showing lowest lying levels.

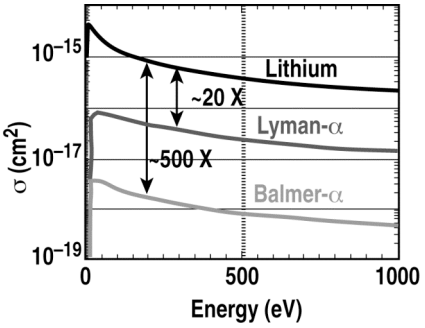

FIGURE 3. Electron excitation cross sections leading to emission for temperatures characteristic of the pedestal region. Black: Li ^2P-^2S; dark gray: H ^2P-^1S (Lyman-alpha); light gray: H 3-2 (Balmer-alpha).

2.3. Zeeman Effect

In the magnetic fields typical of most modern tokamaks (B > ~1 T), the spectral line emission is split and shifted by the Zeeman effect due to spin-orbit interaction with the field, with the shift and polarization of the components being determined by the field strength B and the change in magnetic quantum number Δm [4,5]. At these field levels the lithium ^{2}P levels are fully mixed (Paschen-Back regime) and the resonance emission forms a Lorenz triplet. The shift in wavelength for the two σ lines is given by $\Delta\lambda_B = \Delta m(\mu/hc)\lambda_0^2 B$ (Fig. 4). For the lithium resonance wavelength the shift is 0.021 nm/T.

For each of the three Zeeman components, the emission has unique polarization characteristics: for emission perpendicular to B, the π line (Δm = 0) is linearly polarized parallel to the direction of B and the two σ lines (Δm = ±1) are linearly polarized perpendicular to B (Fig. 5). For emission parallel to B, there is no π emission, and the two σ states exhibit circular polarization, with the shorter wavelength σ- being left-circularly polarized and the longer wavelength σ+ being right-circularly polarized. For the general case of emission in an arbitrary direction with respect to **B**, the emission **I** of the [π, σ+, σ-] manifold can be expressed in matrix form [6,7] in terms of the Stokes parameters [S0, S1, S2, S3] [8] as a function of two angles α and γ:

$$I = \left[[I\pi] + [I\sigma-] + [I\sigma+] \right] = I_0 \left[\begin{bmatrix} \frac{\sin^2\alpha}{2} \\ \frac{\sin^2\alpha\cos(2\gamma)}{2} \\ \frac{\sin^2\alpha\sin(2\gamma)}{2} \\ 0 \end{bmatrix} + \begin{bmatrix} \frac{1+\cos^2\alpha}{4} \\ -\frac{\sin^2\alpha\cos(2\gamma)}{4} \\ -\frac{\sin^2\alpha\sin(2\gamma)}{4} \\ \frac{\cos\alpha}{2} \end{bmatrix} + \begin{bmatrix} \frac{1+\cos^2\alpha}{4} \\ -\frac{\sin^2\alpha\cos(2\gamma)}{4} \\ -\frac{\sin^2\alpha\sin(2\gamma)}{4} \\ -\frac{\cos\alpha}{2} \end{bmatrix} \right] \quad . (1)$$

In the above expression α is the angle between the view chord and the field and γ is the projection of the field inclination angle B_{POL}/B_{TOR}.

2.4. Electric Field Insensitivity

Because of the large energy separation of the lithium 2p levels, there is essentially no measurable Stark effect (intrinsic or motional) on the spectra, even for high velocity beams. Thus the polarization and wavelength effects are due strictly to the magnetic field.

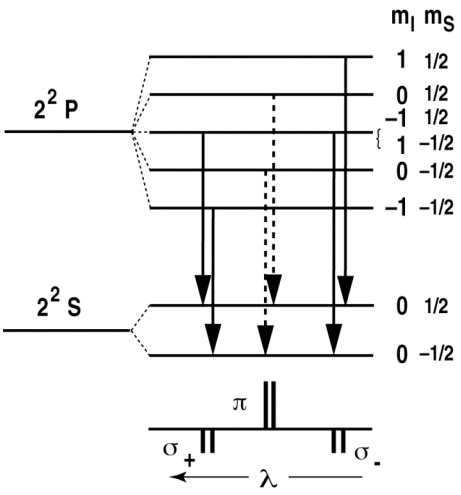

Figure 4. Lithium levels and allowed transitions for normal Zeeman (Paschen-Back) regime in lithium. The lower graph shows the polarization associated with each of the transitions.

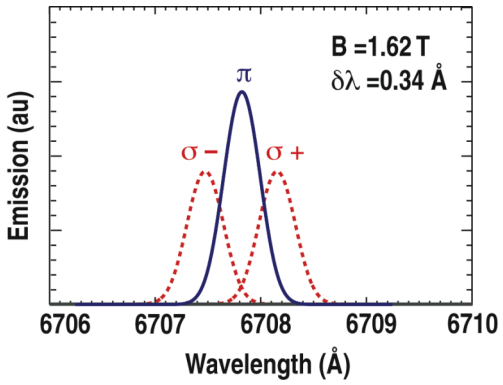

Figure 5. Lithium line emission profile calculated for a position near the outside midplane of DIII-D for a 2.1 T, 1.86 MA plasma. An estimated transverse beam temperature of 1.0 eV was used to calculate the Doppler broadening of the line components. The distance between the two σ peaks for this example (total B = 1.62 T) is 0.068 nm.

2.5. Monoenergetic Beam Formation and Neutralization

To take advantage of the polarization behavior, the Doppler broadening of the emission must be minimized compared to the Zeeman splitting. For a transverse beam view this sets stringent limits on beam divergence and monoenergeticity. The existence of effective thermo-emissive lithium ion sources based on aluminosilicates [9,10] permits the creation of high brightness, single isotope beams having a fraction of the energy spread of plasma discharge type sources. In addition, the extremely high efficiency for charge transfer for lithium on sodium vapor allows us to obtain ~90% neutralization efficiency within a very short neutralization distance. This minimizes the space charge emittance growth in the beam that adds to Doppler broadening. Specific techniques are discussed in Sec. 4.

3. METHOD OF INTERPRETATION

There are a number of ways to utilize these atomic properties to infer the local magnetic field components, and hence j, from the fluorescence emission. Prior analysis techniques have included linear polarization analysis of the collisional fluorescence [11,12] enhancement and polarization-dependent pumping using a resonant laser to induce fluorescence [13], line scanning and modulation of the circular polarization to identify parallel field components [14], and precision line profile intensity measurements to take advantage of the known sigma/pi variation with field direction [15,16]. In each case, the goal is to identify ratios of the various terms in Eq. (1).

In the present case, because we wish to achieve the highest possible radial resolution and sensitivity to the poloidal field component, we have chosen a viewing geometry that is: (1) tangent to the magnetic flux surfaces, (2) orthogonal to the beam, and (3) normal to the toroidal magnetic field (Fig. 6). Given this geometry, analysis of

one of the sigma states yields the field direction by identifying the ratio of circular to linear polarization:

$$\frac{S_3}{\left(S_1^2 + S_2^2\right)^{1/2}} = \frac{2\ \cos\alpha}{1 - \cos^2\alpha} \quad . \tag{2}$$

This measurement is sufficient to interpret B_{POL}, given the known toroidal field and viewing geometry from a spatial calibration [17].

4. HARDWARE REQUIREMENTS AND THE DIII-D LIBEAM SYSTEM

There are five primary requirements that must be must be satisfied in order to provide a useful measurement based on the above atomic physics: (1) a beam of sufficient intensity to allow the desired time and spatial resolution with minimal Doppler broadening, (2) a suitable array of viewing points along the beam with the requisite angular acceptance, along with an accurate spatial calibration of the viewing geometry, (3) minimization and characterization of any unwanted systematic polarization effects in the optical system, (4) a high efficiency, narrow band optical filter which passes the desired Zeeman component while providing sufficient spectral rejection of the remainder of the line profile to ensure a reasonable level of polarization, and (5) a method of accurately analyzing the resulting time-dependent polarization. The LIBEAM system on DIII-D has been developed to satisfy each of these requirements; the progressive improvements in hardware and performance have been documented in detail in several previous publications [6,7,18-22]. Briefly, the system (Fig. 6) comprises a 30 keV, 10 mA neutral equivalent lithium beam of approximately 1.5 cm diameter and an imaging system which collects 32 channels of finely spaced ($\delta R \sim 0.5$ cm) beam emission from the edge region of DIII-D. The beam is formed using a 5 cm diameter ^{6}Li ion emitter, focused into a 1 cm beam, then neutralized in a small sodium vapor cell. The lighter isotope is used to achieve slightly higher beam velocity and better plasma penetration for a given accelerator voltage. The fluorescent emission from the collisionally excited neutral lithium beam is transmitted through dual photoelastic modulators (PEMs) [23] that modulate the polarization of the input light at multiples of the two drive frequencies (20.1, 23.1 kHz). A linear polarizer immediately after the PEM pair transforms the polarization modulation into amplitude modulation and the fluorescence from each spatial location is transmitted through optical fibers to the detector room. The output of each fiber is filtered using individual doubled etalon narrowband (~0.03 nm) filters that are temperature-tuned to the Doppler-shifted σ- line for each view. The shorter-wavelength σ- line is chosen because the longer wavelength is slightly contaminated by emission from a small amount (~4%) of ^{7}Li in the beam. A 1.0 nm bandpass filter in series with the etalons suppresses the plasma background light. The modulated light signals are then detected using a high quantum-efficiency photomultiplier tube-transimpedance amplifier combination. The 32 individually tuned channel outputs are digitized during each tokamak discharge at up to 300 kHz, along with the two PEM

drive frequencies. Details of the digital lock-in analysis used to extract cos α, along with the calibration procedures used to correct for non-perfect filtering of the σ- line by the etalons are given in Ref. 13.

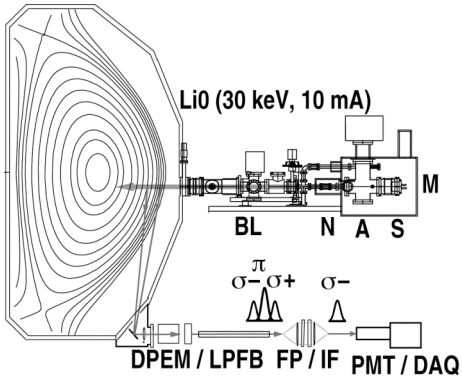

Figure 6. The LIBEAM system on DIII-D, showing the accelerator and schematic of optical system. S=^{6}lithium ion source, A= electrostatic accelerator, N=sodium vapor neutralizer cell, M=magnetic shielding, BL=beamline, DPEM=dual photoelastic modulator, LP=linear polarizer, FB=32 element fiber bundle, FP=dual element, temperature tuned Fabry-Perot etalon (32 channels), IF=1 nm lithium line interference filter, PMT=GaAs photomultiplier tube, DAQ=data acquisition and analysis computer.

5. SOME RECENT RESULTS OF EXPERIMENTS ON DIII-D

In this section we show a few physics results from DIII-D demonstrating the effectiveness of this technique for determining edge current behavior. Figure 7 from Ref. 25 shows the measured poloidal field profile for conditions having low and high edge pedestals. The existence of an edge current is obvious from the large relative change in the field in the region just inside the last closed flux surface. Figure 8 from Ref. 24 shows the inferred current densities using Ampere's law [26] for the two cases. Note the extremely peaked, cm scale current density in the H-mode case.

Calculated values for the expected neoclassical currents [27,28] based on the measured pressure profiles are in good agreement with the measured one. Further measurements [25,29] have confirmed that the location of the current peak is coincident with the peak in the edge pressure gradient, and that the time evolution of

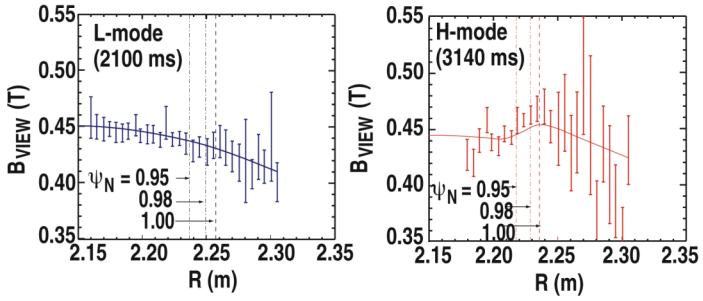

Figure 7. Edge profiles of B_{VIEW} for DIII-D discharge 115114 for times having low and high pedestal pressures. B_{VIEW} is the magnetic field component parallel to the diagnostic sightlines and is essentially the poloidal field because of the arrangement of the viewchords. The location of the last closed flux surface is indicated by the vertical dotted line =1.00, where Ψ_N is the normalized poloidal flux. Adapted from Ref. 25. Solid curves are profiles from an equilibrium reconstruction.

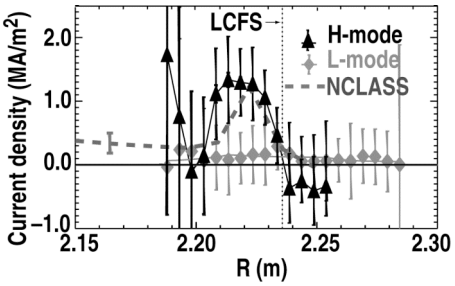

Figure 8. Value of the edge toroidal current density for L-mode (gray) and H-mode (black) on DIII-D shot 115114. Dashed curve is toroidal current density calculated using NCLASS model and measured pressure profiles. LCFS = last closed flux surface. Adapted from Ref. 24.

the current also follows the pressure gradient growth, as expected by theory. Evaluation of the current for different plasma edge densities and temperatures shows a decrease in the edge current density as the plasma collisionality ($\sim n/T^{3/2}$) increases [30], also in accord with theory. Finally, recent efforts to improve the time resolution through conditional averaging techniques have succeeded in showing some features of the magnetic field evolution in between periodic MHD relaxation events in the edge, where plasma confinement is transiently reduced, then restored [31].

6. DISCUSSION AND CONCLUSION

As presently deployed, the LIBEAM diagnostic is a powerful tool for making precise measurements of the local magnetic field structure in the edge of fusion-grade plasmas. This is because of a fortunate coincidence of physical scales, cross sections, and field strengths in existing machines. These measurements have confirmed the existence of large localized currents and are helping to understand the role of these current in pedestal stability and their importance in various toroidal confinement operating regimes. However there are limitations on the time resolution that can be achieved for a given precision. These are primarily set by statistical considerations. In addition, there are several systematic effects — particularly the effect of imperfect spectral filtering and residual polarization — that need to be carefully controlled in order to achieve accurate measurements. We conclude with several improvements that can be made on future experiments that would significantly improve the performance, and hence the utility, of this technique.

First, an improved ion beam current would help on the signal to noise. This can be done through better ion optics design, coupled with a modest increase in beam energy (~30%) that would improve the beam emittance without materially decreasing the effective neutralization efficiency. The higher beam energy would also give better penetration and would decrease the error bars inside of the pedestal region.

Second, beam modulation would help correct for systematic errors in the background light level, which has a small effect on interpreting the proper polarization ratio under low-signal conditions.

Third, an improvement in the quantum efficiency of the detector is desirable. This is straightforward to implement with at least a factor of 3 to 4 improvement possible

using silicon detectors. Care needs to be taken to couple the detectors with the appropriate low-noise preamplifiers to maximize the overall improvement.

Next, measurements using complimentary viewing geometry would help. By choosing different views of the beam, the systematic effect of imperfect filtering can be minimized since the new views will yield different values for the ratio of circular to linear polarization. It might be possible to examine strictly linear polarization by arranging views that intersect the beam but are more or less normal (as opposed to tangential) to the flux surfaces. This would essentially eliminate one class of systematic effects. The decrease in radial resolution might be tolerable, depending on the beam thickness and orientation.

Finally, while the existing magnetic field on the outside midplane of DIII-D (~1.5 T) is sufficient to fully split the Zeeman levels, they are marginally resolved by the existing combination of filtering (etalon performance) and beam performance (Doppler broadening). Even a modest (~50%) increase in the magnetic field strength would improve the situation enormously with no other changes to the hardware by decreasing the bleedthrough of unwanted components. This could be achieved on DIII-D by moving from the outside midplane to the top of the machine (because of the ~1/R dependence of B) or by operation on other devices having higher fields.

ACKNOWLEDGMENTS

This work was supported by the US DOE under DE-AC03-89ER51114 and DE-FC02-04ER54698. D.M. Thomas would like to acknowledge the friends and coworkers that have labored on various aspects of this problem for many years: K. McCormick, W.P. West, A.W. Leonard, R.J. Groebner, R.M. Patterson, J. Kulchar, D. Sundstrom, A. Bozek, J.I. Robinson, K.H. Burrell, T.N. Carlstrom, T.H. Osborne, R.T. Snider, D.K. Finkenthal, R. Jayakumar, M.A. Makowski, D.G. Nilson, B.W. Rice, J.J. Peavy, W.P. Cary, D.H. Kellman, D.M. Hoyt, S.W. Delaware, S.G.E. Pronko, T.E. Harris, P.B. Snyder, T.A. Casper, L.L. Lao, P. Gohil, H.W. Mueller, and M.E. Fenstermacher. The enduring support and encouragement of T.S. Taylor and R.D. Stambaugh, is also gratefully acknowledged.

REFERENCES

1. F. M. Levinton, *et al.*, "Magnetic Field Pitch-Angle Measurements in the PBX-M Tokamak Using the Motional Stark Effect," *Phys. Rev. Lett.* **63**, 2060 (1989).
2. B. W. Rice, *et al.,* "Effect of Plasma Radial Electric Field on Motional stark Effect Measurements and Equilibrium Reconstruction," *Nucl. Fusion* **37**, 517 (1997).
3. J. Schweinzer, *et al.,* "Database for Inelastic Collisions of Lithium Atoms With Electrons, Protons and Multiply Charged Ions," *At. Data Nucl. Data Tables* **72**, 239-273 (1999).
4. E. U. Condon and G. H. Shortley, *The Theory of Atomic Spectra*, Cambridge University Press, 1963, 149 ff.
5. H. A. Bethe and E. E. Salpeter, *Quantum Mechanics of One- and Two-Electron Atoms*, Plenum, 1977, 205 ff.
6. D. M. Thomas, *et al.,* "Prospects for Edge Current Density Determination Using LIBEAM on DIII-D," *Rev. Sci. Instrum.* **72**, 1023-1027 (2001).
7. D. M. Thomas, "Poloidal Magnetic Field Measurements and Analysis With the DIII-D LIBEAM System," *Rev. Sci. Instrum.* **74**, 1541-1457 (2003).

8. D. S. Kliger, *et al., Polarized Light in Optics and Spectroscopy*, Academic Press, 1990, 75 ff.
9. O. Heinz and R. T. Reaves," Lithium Ion Emitter for Low Energy Beam Experiments," *Rev. Sci. Instrum.* **39**, 964-967 (1968).
10. R. K. Feeney, *et al.,* "Alumino-silicate sources of Positive Ions for Use in Collision Experiments," *Rev. Sci. Instrum.* **47**, 964-967 (1976).
11. K. McCormick, *et al.,* "Temporal Behavior of the Plasma Current Distribution in the ASDEX Tokamak During Lower-Hybrid Current," *Phys. Rev. Lett.* **58**, 491-494 (1987).
12. K. Kadota, *et al.,* "Space-resolved Measurement of Internal Magnetic Field in a Bumpy Torus by Li0-beam Probe Spectroscopy," *Rev. Sci. Instrum*. **56**, 857-859 (1985).
13. W. P. West, *et al.,* "Measurement of the Rotational Transform at the Axis of a Tokamak," *Phys. Rev. Lett.* **58**, 2758-2761 (1987).
14. L. K. Huang, *et al.,* "Safety Factor on the Axis of a Tokamak During Ohmically Heated Sawtoothing Discharges from a Localized Measurement of Circular Polarization of the Li 6708 A Line," *Phys. Fluids* **B2**, 809-814 (1990).
15. A. Korotkov, *et al.,* "Line Ratio Method for Poloidal Magnetic Field Measurements Using Li-multiplet (22S-22P) Emission," in *Advanced Diagnostics for Magnetic and Inertial Fusion*, edited by P.E. Stott, *et al.,* Kluwer Academic/Plenum Publishers, New York, 2002, pp. 209-212.
16. A. A. Korotkov, *et al.,* "Line Ratio Method for Measurement of Magnetic Field Vector Using Li-multiplet (22S–22P) Emission," *Rev. Sci. Instrum.* **75**, 2590-2602 (2004).
17. D. M. Thomas and A. W. Leonard, "Signal Processing Techniques for Lithium Beam Polarimetry on DIII-D," *Rev. Sci. Instrum.* **77**, 10F515-1:4 (2006).
18. D. M. Thomas, *et al.,* "Low-divergence, High Brightness Lithium Ion Source for Plasma Diagnostics," *Rev. Sci. Instrum.* **59**, 1735-1737 (1988).
19. D. M. Thomas, "Development of Lithium Beam Spectroscopy as an Edge Fluctuation Diagnostic for DIII-D," *Rev. Sci. Instrum.* **66**, 806-811 (1995).
20. D. M. Thomas, *et al.,* "Utilization of LIBEAM Polarimetry for Edge Current Determination on DIII-D," in *Advanced Diagnostics for Magnetic and Inertial Fusion*, edited by P.E. Stott, *et al.,* Kluwer Academic/Plenum Publishers, New York, 2002, pp. 319-322.
21. T. N. Carlstrom, *et al.,* "Optical Design for Li Beam Polarimetry Measurements on DIII-D," *Rev. Sci. Instrum*. **74**, 1601-1604 (2003).
22. J. J. Peavy, *et al.,* "Control System for the Lithium Beam Edge Plasma Current Density Diagnostic on the DIII-D Tokamak," Proc. 20th IEEE/NPSS Symp. on Fusion Engineering, IEEE, Piscateway, New Jersey, 2003, pp. 344-346.
23. J. C. Kemp, *Polarized Light and its Interaction with Modulating Devices - A Methodology Review*, Hinds International, Hillsboro, Oregon, 1987.
24. D. M. Thomas, et al., "Measurement of Pressure-Gradient-Driven Currents in Tokamak Edge Plasmas," *Phys. Rev. Lett.* **93**, 0650031-4 (2004).
25. D. M. Thomas, *et al.,* "Measurement of Edge Currents in DIII-D and Their Implication for Pedestal Stability," *Phys. Plasmas* **12**, 056123-1 (2005).
26. D. M. Thomas, *et al.,* "Calculation of Edge Toroidal Current Density Distributions from DIII-D Lithium Beam Measurements Using Ampere's Law," *Rev. Sci. Instrum.* **75**, 4109-4111 (2004).
27. W. A. Houlberg, *et al.,* "Bootstrap Current and Neoclassical Transport in Tokamaks of Arbitrary Collisionality and Aspect Ratio," *Phys. Plasmas* **4**, 3230 (1997).
28. O. Sauter, *et al.,* "Neoclassical Conductivity and Bootstrap Current Formulas for General Axisymmetric Equilibria and Arbitrary Collisionality Regime," *Phys. Plasmas* **6**, 2834 (1999).
29. D. M. Thomas, *et al.,* "Edge Currents and Stability in DIII-D," Proc. 31st EPS Conf., European Physical Society, London, 2004, Paper P2-177.
30. D. M. Thomas, *et al.,* "The Effect of Plasma Collisionality on Pedestal Current Formation in DIII-D," *Plasma Phys. Control. Fusion* **48**, A183-A191 (2006).
31. D. M. Thomas, *et al.,* "Edge Current Growth and Saturation During the Type 1 ELM Cycle," Proc. 33st EPS Conf., European Physical Society, Roma, 2006, ECA Vol. 301, Paper P5-139.